行政院國家科學委員會專題研究計畫成果報告

以奈米孔陽極氧化鋁(AAO)版模法製作電子場發射奈米結構材料（3/3）

計畫類別： 個別型
計畫編號： NSC 96-2221-E-009-109-MY3
執行期間： 98 年 08 月 01 日至 99 年 07 月 31 日

計畫主持人： 潘扶民教授 國立交通大學材料科學與工程學系
計畫參與人員： 陳重守 張智傑 吳姿慧

一、中文摘要

本研究利用奈米多孔性的陽極氧化鋁薄膜(AAO)做為模板製備出高規則的各種奈米結構陣列，包括奈米碳管(CNT)，Si，TiO_2與非晶質碳奈米尖錐陣列，探討該等奈米結構陣列的場發射特性，為了優化奈米碳管陣列的場發射特性，我們亦研究CNT在侷限的AAO孔洞中之成長機制，本成果報告即就此研究結果提出說明，我們發現利用電漿輔助化學氣相沉積法在AAO中成長CNT時，鈷催化劑奈米顆粒可能以毛細作用力，沿著AAO管壁上升，而在熔融態鈷催化劑顆粒內的過飽和碳原子析出，在催化劑底部形成CNT，於是成為CNT頂端(tip)成長型態。

關鍵詞：陽極氧化鋁、奈米結構、電子場發射，奈米碳管，鈷

Abstract:

The study prepared anodic aluminum oxide (AAO) thin films as a template for fabrication of various highly ordered nanostructure arrays, including carbon nanotubes (CNT) and silicon,TiO_2 as well as α-carbon nanocone arrays. We studied electron field emission characteristics of these nanostructured materials. To optimize the field emission property of CNT arrays, we studied the growth mechanism of CNTs deposited in confined AAO pore channels by plasma enhanced chemical vapor deposition. We found that liquefied Co catalyst nanoparticles were lifted along the pore surface of AAO channels by capillary force during the CNT growth. Saturated carbon in the Co particle segregated to the bottom surface of the particle, thereby forming carbon nanotubes via the tip grown mode.

Keywords: anodic aluminum oxide, nanostructure, field emission, carbon nanotube, cobalt.

1. Introduction

For many technical applications of carbon nanotubes (CNTs) and nanofibers (CNFs), such as interconnects for integrated circuits [1], CNT purification by zeolite supports [2] and field emission emitters [3,4], CNTs/CNFs are required to be selectively grown in a confined region. Unlike CNT/CNF growth in an open space, the geometric configuration of a confined space will restrain transport behavior of the precursor gas species and the catalyst area directly exposed to the precursors, thereby resulting in a growth kinetics different from CNT/CNF growth on a blank substrate. This is more likely to occur to CNTs/CNFs growth by plasma-assisted chemical vapor deposition (PACVD). Because of the applied sample bias and reactive radicals as well as ionic species, etch and deposition of graphitic structure and carbonaceous residue under a typical PACVD condition can be greatly affected by the spacial geometry. In this study, we grew CNTs/CNFs in the AAO template by electron cyclotron resonance chemical vapor deposition (ECR-CVD), and studied the size effect of the Co catalyst on CNT/CNF growth in the pore channel. A CNT/CNF growth mechanism in the AAO pore channel is proposed.

2. Experimental

The preparation of the AAO template was started with sputter depositing an aluminum thin film 2μm thick on the 4 in Si wafer. To prepare highly aligned AAO pore channels, two-step electrochemical anodization was performed. The detail of the anodization procedure has been previously described [5,6]. After the second anodization step, a 200 nm thick Al layer was deliberately remained beneath the AAO template, and used as the substrate for Co catalyst electrodeposition. To deposit CNFs in the AAO template, the Co catalyst was first treated with the H_2 plasma at 600°C for 10 minutes in the ECR-CVD system. CNF growth was then carried out in a gas mixture of CH_4 and H_2 (5 sccm/ 25 sccm) at 600°C for 35 minutes under the following growth conditions: power 750 W, substrate bias -100 V, working pressure ~2×10^{-3} torr.

3. Results and Discussion

Figure 1 shows the side-view SEM images of

CNFs grown out of the AAO template with Co catalysts electrodeposited for various times. For samples with Co catalysts deposited for 45 and 60 sec (Figs. 1(a) and (b)), CNFs had irregular shapes with a sparse tube density and a diameter smaller than the AAO pore size. On the other hand, as the catalyst deposition time increased to 75 and 90 sec (Figs. 1(c) and (d)), well aligned CNFs were grown out over the AAO surface with a tube diameter close to the AAO pore size. From Figs 1(a) and (b), a residual deposit can be clearly seen to cover a large area of the AAO surface. Raman spectra (not shown) showed that a significant amount of α-carbon was deposited on the AAO template during the CNF growth. The α-carbon was heavily deposited around CNFs, but became scarce away from the CNFs. This suggests that the CNF growth was accompanied by concurrent α-carbon deposition in the AAO pore channel.

Figure 2 shows the cross-sectional SEM images of CNFs grown in the AAO template. CNFs grown with a smaller Co particle size were seriously distorted in shape and some were buried in the AAO pore channels (marked by circles) as shown in Fig. 2(a) for the Co catalyst deposited for 60 sec. Many CNFs extending out of the AAO pores had a gradual decrease in the tube diameter along the tube shaft. It can be clearly seen that CNF shafts inside the pore channels were embedded by lumps of precipitate (marked by arrows). On the other hand, according to Fig. 2(b), CNFs grown with the Co catalyst deposited for 90 sec had the growth direction in the AAO template much more compliant with the pore channel, and became highly aligned after extending out of the pore. Figure 2(c) shows the SEM image of the AAO template treated with the same CNF deposition condition but without the Co catalyst. The pore wall was very smooth and the top portion of the AAO exhibited a clean but jagged feature. This suggested that the surface region was subject to plasma etch during the PACVD process. It have been reported that CNFs could be grown in the AAO template without metallic catalysts [7,8]. However, no CNF growth was observed in the study. The observation implied that the Co particle played a major role not only catalyzing the CNF growth but also facilitating deposition of the α-carbon residue.

The TEM image of an FIB prepared sample with the Co catalyst deposited for 90 sec is shown in Fig. 3(a). It can be clearly seen that cone-shaped catalyst particles were present at the tip of the CNFs, indicating that the CNF growth in the AAO template was via the tip-growth mode. Co particle fragments were also observed inside the CNF shaft. Figure 3b shows the TEM image of CNFs grown with the Co catalyst deposited for 90 sec. Some Co particles were stuck to the root of the CNFs. They were likely those originally left at the AAO pore bottom during the CNF growth. The inset is a high-resolution TEM (HRTEM) image for the area near the tip of a CNF grown. A disordered amorphous layer was present on the tube surface. The CNF was ~55 nm in diameter and had 61 well-ordered graphitic layers, which had the interlayer distance of ~3.7 Å, near the bottom of the catalyst particle. For comparison, CNFs grown with Co deposited for 60 and 75 sec had ~34 and ~53 graphene layers, respectively.

The vapor-liquid-solid model is a commonly accepted CNT/CNF growth mechanism, which suggests that carbon diffusion in the liquefied metal catalyst is a required step for CNF growth. The cone-shaped catalyst and the segmentation of Co particles shown in the TEM images is an implication of Co liquefaction during the CNF growth in the AAO template. It has been proposed that a temperature gradient can be developed in the catalyst particle as the concentration distribution of the dissolved carbon is nonuniform in the particle [9]. The catalyst has a higher temperature in the region supersaturated with carbon, and graphene sheets grow from the region with a smaller carbon concentration. We thus propose that the particle segmentation probably resulted from the temperature gradient developing in the Co particle [10]. Because Co has a reasonable wetting strength with aluminum oxide [11,12], it was likely that capillary force might initially assist lifting the liquefied Co particle, and thus allow developing an open space for carbon precipitation for graphitic sheet formation. As the liquefied Co particle moved upward with the growing CNF shaft, the particle was eventually separated leaving the unliquefied part at the bottom of the AAO pore channel.

As discussed above, CNF growth on the AAO template was accompanied by deposition of α-carbon, and more α-carbon was deposited for a smaller Co particle. The α-carbon accumulation on the pore wall surface could hinder the motion of the liquefied catalyst particle in the pore channel, thereby changing the moving direction and geometric shape of the catalyst during the CNF growth. This can explain why most CNFs grown under a condition of heavy α-carbon deposition showed a twisted feature inside the pore channels and had a fiber diameter smaller than the AAO pore size. In addition, from Fig. 3b, many nanosized particles, probably Co, adhered to the tube surface of the CNFs. It is likely that the rough wall surface of the AAO pore channel, due to the α-carbon deposition, disturbed the movement of the liquefied Co particle with the growing CNF, thereby chipping off the surface layer of the Co catalyst particle. The chipped off nanoparticles could then adhere to the surface of the growing CNFs and moved upward accordingly.

The growth mechanism of CNFs in AAO pore channels is schematically illustrated in Fig. 4. Because the AAO pore channels not only limit the flow direction and flux of the plasma species toward the Co catalyst but also define the exposing area of the Co particle, the impinging rate of carbonaceous and hydrogen radicals and ions onto the catalyst surface should be independent of the Co particle size. Once adsorbed and decomposed on the Co catalyst surface, carbon species may diffuse on the surface or dissolve into the particle. The Co particle becomes supersaturated with carbon on the top region earlier than the lower part, resulting in the development of a temperature gradient in the particle and thus Co liquefaction occurs earlier in the top region. Initially, the liquefied Co may be driven by capillary force to move upward in the AAO pore channel, leading to segmentation of the Co particle. Carbon atoms precipitating at the bottom of the liquefied Co segment then grow into graphitic sheets, forming carbon nanofibers in the AAO pore channel via the tip-growth mode. As CNFs begin to grow, Co particle may be pushed upward by the fiber skeleton for further CNF growth. Because etching the α-carbon deposit by plasma species is not effective in the pore channel due to the high aspect ratio, carbonaceous deposit cannot quickly removed away from the surface. Carbon dissolves into the Co particle is the only pathway for reducing surface concentration of the carbon deposit. Because carbon becomes saturated more quickly in the smaller particle than the bigger one as discussed before, more α-carbon may be left on the particle surface. If the α-carbon deposition prevails over CNF growth, extensive α-carbon accumulation can occur on the top of the catalyst and the pore wall, thus retarding the CNF growth. The α-carbon deposit can modify the geometric shape of the liquefied catalyst and thus diminish active catalytic area, thereby leading to growth of CNFs with a smaller diameter and a distorted shape. In the extreme situation, the pore opening may be completely blocked by the α-carbon deposit before the CNF grows out of the pore, thus terminating the inflow of the precursor species and stopping the CNF growth. On the other hand, the bigger Co particle dissolves more carbon atoms and, therefore, accumulation of α-carbon on the surface can be effectively diminished, making CNF growth in the pore channel easier.

4. Conclusion

CNFs were grown in the AAO template by ECR-CVD using electrodeposited cobalt as the catalyst. The tube density, diameter and tube alignment of CNFs grown in AAO pore channels strongly depended on the size of the electrodeposited Co particle. Carbon dissolution in the Co particle at the bottom of the pore channel induced a temperature gradient and Co melting in the particle, leading to the segmentation of the Co particle in the AAO pore channel. When the Co catalyst particle was small, heavy deposition of α-carbon took place in the pore channel under the plasma assisted CVD condition, and the CNF growth was adversely affected. A growth mechanism was proposed to delineate the effect of the Co catalyst size on the CNF growth in the AAO pore channels.

References

[1] Kreupl F, Graham AP, Duesbger GS, Steinhögl W, Liebau M, Unger E, et al. Carbon nanotubes in interconnect applications. Microelectronic Eng 2002; 64(1-4): 399-408.

[2] Hernadi K, Fonseca A, Nagy JB, Bernaerts D, Fudala A, Lucas AA. Catalytic synthesis of carbon nanotubes using zeolite support. Zeolites 1996; 17(5-6): 416-23.

[3] Lin CC, Chang KC, Pan FM, Kuo CT, Liu M, Mo CN. Growth of carbon nanotube field emitters in the triode structure using anodic aluminum oxide as the template. Diamond & Related Materials 2007; 16(4-7): 1388-92.

[4] Van Quy N, Hoa ND, An M, Cho Y, Kim D. A high-performance triode-type carbon nanotube field emitter for mass production. Nanotechnology 2007; 18(34): 345201.

[5] Chen PL, Chang JK, Kuo CT, Pan FM. Field emission of carbon nanotubes on anodic aluminum oxide template with controlled tube density. Appl Phys Lett 2005; 86(12): 123111.

[6] Chen PL, Kuo CT, Tsai TG, Wu BW, Hsu CC, Pan FM. Self-organized titanium oxide nanodot arrays by electrochemical anodization. Appl Phys Lett 2003; 82(17): 2796-8.

[7] Lee JS, Gu GH, Kim H, Jeong KS, Mae J, Suh JS. Growth of carbon nanotubes on anodic aluminum oxide templates: fabrication of a tube-in-tube and linearly joined tube. Chem Mater 2001; 13(7): 2387-91.

[8] Yao BD, Wang N. Carbon nanotube arrays prepared by MWCVD. J Phys Chem B 2001; 105(46): 11395-8.

[9] Kanzow H, Schmalz A, Ding A. Laser-assisted production of multi-walled carbon nanotubes from acetylene. Chem Phys Lett 1998; 295(5-6): 525-30.

[10] Harutyunyan AR, Tokune T, Mora E. Liquefaction of catalyst during carbon single-walled nanotube growth. Appl Phys Lett 2005; 86(15): 153113.

[11] Wang XG, Smith JR. Hydrogen and carbon effects on Al_2O_3 surface phases and metal deposition. Phys Rev B 2004; 70(8): 081401.

[12] Chambers SA, Droubay T, Jennison DR, Mattsson TR. Laminar growth of ultrathin metal films on metal oxides: Co on hydroxylated α-Al_2O_3(0001). Science 2002; 297(5582): 827-31.

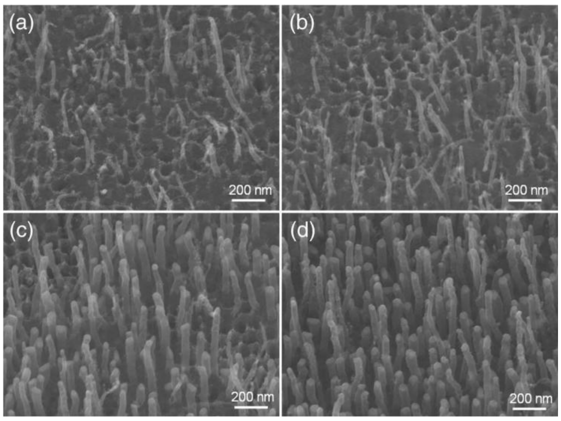

FIG. 1. SEM images of CNFs grown for 35 min on the AAO template with different Co catalyst sizes: (a) 45 sec; (b) 60 sec; (c) 75 sec; and (d) 90 sec.

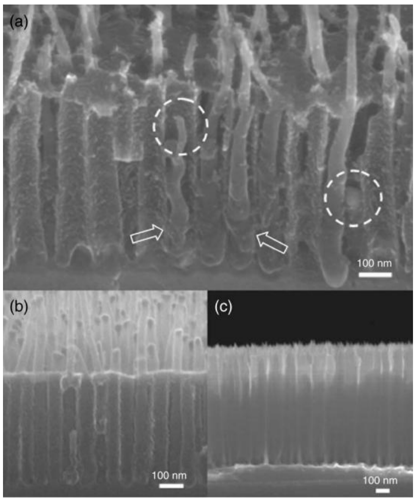

FIG. 2. (a) Side view SEM image of CNFs grown for 35 min in the AAO template with Co catalyst deposited for 60 sec. CNFs capped by the surface α-carbon layer were marked by circles, and α-carbon deposits embedding CNFs were marked by arrows; (b) and (c) are cross sectional SEM images for CNF grown for 35 min on the AAO template with Co catalyst deposited for 90 sec and without the Co catalyst, respectively.

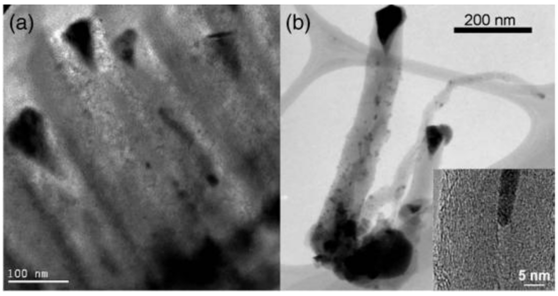

FIG. 3. TEM images of CNFs grown with the Co catalyst deposited for 90 sec: (a) an FIB prepared sample of which CNFs were inside the AAO pore channels; (b) CNFs separated from AAO pore channels by ultrasonic agitation. The inset is the high resolution TEM image of the area near the tip of a CNF.

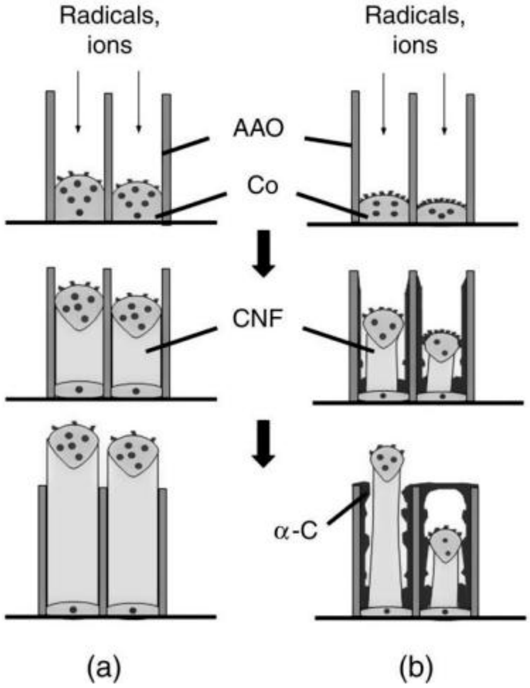

FIG. 4. Schematic illustration of CNF growth mechanism in the AAO pore channel: (a) CNF growth with a large Co catalyst; (b) CNF growth with a small Co catalyst. The dots stand for carbon dissolved in the Co particle, and the number and size of the dots denote the amount of carbon dissolved. Detailed description about the growth mechanism is given in the text.